International Journal of Refrigeration 148 (2023) 131–142

Contents lists available at ScienceDirect

International Journal of Refrigeration

journal homepage: www.elsevier.com/locate/ijrefrig

Energy comparison based on experimental results of a cascade refrigeration system pairing R744 with R134a, R1234ze(E) and the natural refrigerants R290, R1270, R600a

Comparaison énergétique basée sur les résultats expérimentaux d'un système de réfrigération en cascade associant le R744 au R134a, R1234ze(E) et les réfrigérants naturels R290, R1270, R600a

R. Cabello [a,*], A. Andreu-Nácher [a], D. Sánchez [a], R. Llopis [a], F. Vidan-Falomir [a]

[a] *Thermal Engineering Group (GIT), Department of Mechanical Engineering and Construction, Jaume I University, Castellón, E-12071, Spain*

ARTICLE INFO

Keywords:
CO2
R290
R1270
R600a
R1234ze(E)
Energy efficiency
Mots clés:
CO2
R290
R1270
R600a
R1234ze(E)
Efficacité énergétique.

ABSTRACT

Refrigeration architectures for low-temperature applications are gaining interest in the Industrial, Commercial and Health fields. One of the most classical architectures is cascade systems, where two mechanical single vapor compression cycles are thermally paired by the cascade heat exchanger (HX_{cc}). The HX_{cc}, acts as condenser for the low temperature cycle and as evaporator for the high temperature cycle. Each cycle is charged with a different refrigerant adapted to the operating conditions. New environmental rules make necessary to find proper refrigerant pairs to get refrigeration plants with high energy efficiency together with environmentally friendly fluids. This experimental work compares the energy performance of a cascade refrigeration system working with the pair R134a/R744 against four alternative refrigerant pairs: R290/R744, R1270/R744, R600a/R744CO2 and R1234ze(E). Laboratory tests were conducted at three heat rejection temperatures: 20, 30 and 40°C, maintaining a fixed low-temperature heat source level (−20°C). The energy analysis shows that R290/R744 and R1270/R744 improve the cooling capacity at low heat sink temperatures, and the pair R290/R744 improves the energy performance at low temperatures. The environmental analysis shows that all the refrigerant pairs achieve a reduction in CO_{2eq} emissions.

1. Introduction

Cascade refrigeration plants are a classical architecture used to give service to low temperature cooling loads. As the other types of refrigeration plants, they are experiencing the transition to low GWP and high energy performance in accordance with several rules like Kigali amendment to Montreal Protocol (UNEP 2016) or EU n°517/2014 (European-Union 2014), aimed at reducing greenhouse effect.

In the current picture, R744 is almost the unique refrigerant with A1 safety classification, according with ASHRAE std34 classification, suitable to accomplish the above-mentioned rules and, at the same time, able to be used for medium and low evaporating temperature applications. That is the reason why, for commercial refrigeration specially, booster architectures using R744 in supercritical conditions are being mainly studied and developed at this moment. But cascades using R744 in the low temperature circuit are an alternative that deserves some research. Different studies have theoretically evaluated their good performance opposed to booster architectures, both in industrial applications (LUND et al., 2019) as in commercial (Catalán-Gil et al., 2018). The first at high heat sink temperatures and the last at lower heat source temperatures and high heat rejection ones. Also, in other experimentally studies, the better energy performance in warm climates has been measured for typical supermarket and convenience stores (Tsamos et al., 2019)

One of the main research topics related with cascade refrigeration plants designed for commercial applications, is to find the proper refrigerant to be used in the high-temperature cycle when R744 is used

* Corresponding author.
E-mail address: cabello@uji.es (R. Cabello).

https://doi.org/10.1016/j.ijrefrig.2023.01.009
Received 2 June 2022; Received in revised form 9 January 2023; Accepted 11 January 2023
Available online 16 January 2023

Nomenclature

COP	coefficient of performance
GWP_{100}	Global warming potential, 100 years horizon
h	specific enthalpy ($kJ \cdot kg^{-1}$)
HC	Hydrocarbon
HTC	High temperature cycle
HX	Heat Exchanger
LTC	Low temperature cyle
$\dot{m}$	mass flow rate ($kg \cdot s^{-1}$)
p	pressure (kPa)
P_C	Compressor electrical power (kW)
$\dot{Q}$	Heat transfer rate (kW)
q_o	specific cooling capacity ($kJ \cdot kg^{-1}$)
t	Compression ratio (-)
T	temperature, (K or °C)
v	specific volume ($m^3 \cdot kg^{-1}$)
w_c	Specific compression work ($kJ \cdot kg^{-1}$)
x_v	vapour quality

Greek symbols

λ	latent heat of phase-change ($kJ \cdot kg^{-1}$)
Δ	Prefix, means preceding variable variation
d	Uncertainty
η_G	Compressor Global Efficiency

Subscripts

cc	Cascade
dis	Compressor discharge
glyc	Water-Ethilenglycol mixture
H	HTC related parameter
in	Inlet
k	condensing level
L	LTC related parameter
O	evaporating level
o	Outlet
sat,l	saturated liquid
sat,v	saturated vapour
suct	compressor suction
w	Water

in the low temperature one. In this sense, there are theoretical analyses and experimental works. Among the first the work of Zhili et al. (2019) could be highlighted, in which 28 refrigerant pairs are compared using R23, R41 and R170 in the LTC and R32, R1234yf, R1234ze, R161, R1270, R290 and R717 in the HTC, being the pairs R170/R160 and R41/R160 which show better performance. Another theoretical work is that of (Kashra and Kody, 2021), where after compare 18 pairs, pairing R744, R170 and R1150 in the LTC paired with R717, R1234yf, R1234ze, R161, R1270 and R290, in which they found that R170/R160 is the best pair from a thermoeconomic point of view. Among the experimental works that of Makhnatch et al. (2018), could be quoted. They experimentally evaluated the R450A and R513a as substitutes of R134a, finding that R513A provides comparable COP and cooling capacity values to R134a, whereas the cooling capacity and COP of R450A are lower than that of the baseline R134a. Another experimental work to be mentioned is the one of (Sanchez et al., 2019). They explored the energy performance of a direct expansion cascade R134a/R744 converted to an indirect cascade with different refrigerants in the high temperature cycle finding that indirect cascade presents lower energy performance than direct cascade in all tested cases. Also, in the work of (Cabello et al., 2017) the drop-in of R152a in an R134a/R744 cascade plant was investigated, showing an improvement in COP in a wide operating conditions range, but a reduction in cooling capacity.

The main goal of this work is to generate knowledge related to environmentally friendly substitutes for R134a in cascade refrigeration plants. So, the most commercially available refrigerants meeting this criterion, are tested at the HTC against the HFC R134a. They are the hydrocarbons R290, R1270 and R600a, as well as the HFO R1234ze(E). This set of refrigerants are giving good results in other refrigeration applications, so we have tested them in a cascade refrigeration plant using R744 in the LTC to know its energy behavior. The work is completed with a TEWI analysis, where direct and indirect effect in three Spanish locations that characterizes the different climates in this country are estimated. The experimental data presented supposes a contribution to the lack of experimental information in this field. Their analysis shows that all alternative refrigerants tested reduce total CO2eq emissions compared to those generated by R134a. Additionally, the R290 show an slight improve on the energy performance for heat sink temperatures below 30ºC compared to the R134a. Regarding the cooling capacity, only the R1270 gets a notable improvement in the entire heat sink temperature range tested, compared to that obtained with the R134a.

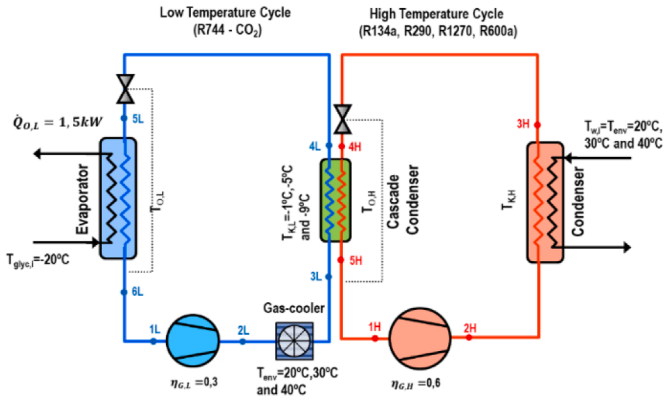

Fig. 1. Simplified plant scheme used for modelling purposes.

2. Preliminary analysis with basic thermodynamic model

We have modelled the cascade plant shown in Fig. 1, to carry out an analysis based on 1st and 2nd thermodynamic laws. The model inlet parameters have been, cooling duty $\dot{Q}_{OL} = 1{,}5$ kW, glycol inlet temperature to evaporator $T_{glyc,i} = -20$ °C, subcooling at condensers outlet 2 K, superheat at evaporators outlet 5 K, superheat in suction lines 15 K. The compressors isentropic efficiencies are considered as constant values for comparison purposes, so $\eta_{is,LTC} = 0{,}3$ and $\eta_{is,HTC} = 0{,}6$. Those values have been adopted because they are similar to the measured ones. Three environmental temperatures have been considered, 20 °C, 30 °C and 40 °C, which are equivalent to three heat rejection temperatures. Correspondingly three condensing temperatures, T_{KL}, have been estimated in the LTC (−1 °C, −5 °C and −9 °C). The other phase change temperatures have been calculated accordingly Eqs. (1) – 3.

Phase change temperatures:

$$T_{O,L} = T_{glyc,i} - 10°C \quad (1)$$

$$T_{k,H} = T_{w,i} + 7°C \quad (2)$$

$$T_{O,H} = T_{k,L} - 5°C \quad (3)$$

Additionally, a 2 K temperature difference between the environmental temperature and the refrigerant gas cooler outlet temperature

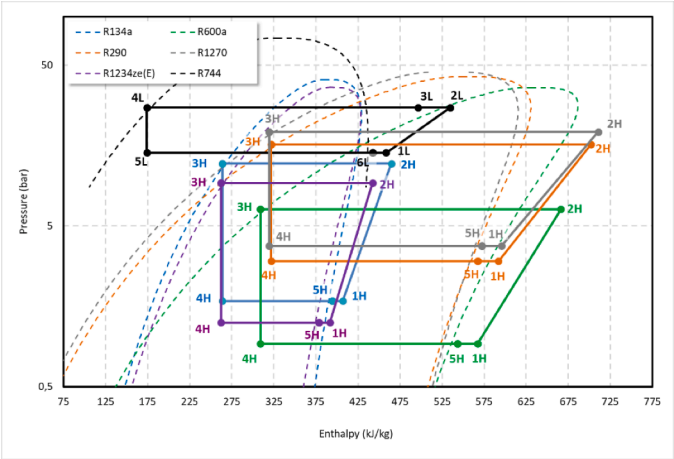

Fig. 2. Comparison of the theoretical cascade cycles with Tenv.; 30°C.

has been considered:

$$T_{3L} = T_{env} + 2°C \tag{4}$$

With the inlet parameters considered, the thermodynamic states that define the cycle shown in Fig. 1, have been calculated using Refprop v10 (Lemmon et al., 2018). Meanwhile, the main energy parameters have been calculated using the set of Eqs. (5) - (19).

$$t_L = \frac{p_{sat}(T_{k,L})}{p_{sat}(T_{O,L})} \tag{5}$$

$$q_{o,L} = h_{6L} - h_{5L} \tag{6}$$

$$\dot{m}_{ref,L} = \dot{Q}_{o,L} \cdot q_{o,L}^{-1} \tag{7}$$

$$\dot{Q}_{k,L} = \dot{m}_{ref,L} \cdot (h_{3L} - h_{4L}) \tag{8}$$

$$w_{c,L} = h_{2L} - h_{1L} \tag{9}$$

$$P_{c,L} = \dot{m}_{ref,L} \cdot (h_{2L} - h_{1L}) \tag{10}$$

$$COP_L = \frac{q_{o,L}}{w_{c,L}} \tag{11}$$

$$t_H = \frac{p_{sat}(T_{k,H})}{p_{sat}(T_{O,H})} \tag{12}$$

$$q_{o,H} = h_{5H} - h_{4H} \tag{13}$$

$$\dot{Q}_{o,H} = \dot{Q}_{k,L} \tag{14}$$

$$\dot{m}_{ref,H} = \dot{Q}_{o,H} \cdot q_{o,H}^{-1} \tag{15}$$

$$w_{c,H} = h_{2H} - h_{1H} \tag{16}$$

$$P_{c,H} = \dot{m}_{ref,H} \cdot (h_{2H} - h_{1H}) \tag{17}$$

$$COP_H = \frac{q_{o,H}}{w_{c,H}} \tag{18}$$

$$COP = \frac{\dot{Q}_{o,L}}{P_{c,H} + P_{c,L}} \tag{19}$$

The resulting thermodynamic cascade cycles calculated at 30 °C of heat sink temperature, are depicted in Fig. 2. We can observe the main differences in pressures, being R600a the refrigerant which operates with the lowest and R1270 with the highest. Also, the differences in the specific cooling capacity, being the R1270 the refrigerant with the highest and R1234ze(E), the one with the lowest. In the case of the specific compression work, it is evidenced that the fluids with lowest and highest values are again R1234ze(E) and R1270, respectively.

The results for all the heat sink temperatures considered are gathered in Table 1. Only the parameters referring to the HTC are commented, since in the theoretical model the LTC is always the same at each heat sink temperature, regardless of the refrigerant used in the HTC. The main comments are regarding to:

- Compressor discharge temperature. R1270 is the one that generates the highest values and R600a the one that generates the lowest. In any case the highest value is above 100 °C, which is a dangerous limit to prevent the lubricant degradation.
- Compression ratio. R1234ze(E) and the R600a are the refrigerants with highest values, meanwhile R134a is the one with the lowest t_H. This means that these refrigerants will need a higher torque on the compressor shaft than the others.
- Specific volume at the compression suction. R600a is the refrigerant with highest value by far, being R134a the one with lowest value. This parameter is related to the size of the tubes and heat exchangers and with the displacement of the compressor.
- Specific cooling capacity. The highest value of this parameter corresponds to the refrigerant R1270 and the lowest one to the refrigerant R1234ze(E). Refrigerants with low specific q_o need to move high refrigerant mass flow rates to match the cooling load.
- Specific compression work. The refrigerant with the highest value is the R1270, on the contrary, R1234ze(E) is the one with the lowest.
- The COP of the HTC (COP_H). Consequently with the $q_{o,H}$ and $w_{c,H}$ values obtained, R600a and R1234ze(E) are the ones with the

Table 1
Theoretical model main results.

Temperature		$T_{dis,H}$ (°C)	$v_{suct,H}$ (m^3/kg)	t_H (-)	t_L (-)	$q_{o,H}$ (kJ/kg)	$q_{o,L}$ (kJ/kg)	$w_{c,H}$ (kJ/kg)	$w_{c,L}$ (kJ/kg)	COP_H (-)	COP_L (-)	COP (-)	ΔCOP (%)
20	R134a/CO_2	58,2	0,1272	4133	1909	159,9	268,2	37,7	76,5	4,24	3,51	1,82	
	R290/CO_2	57,0	0,1636	3318	1909	302,1	268,2	71,1	76,5	4,25	3,51	1,82	0,04
	R1270/CO_2	63,4	0,1368	3231	1909	308,1	268,2	74,8	76,5	4,12	3,51	1,80	−1,43
	R600a/CO_2	49,1	0,4178	4009	1909	284,3	268,2	64,1	76,5	4,43	3,51	1,86	2,09
	R1234ze(E)/CO_2	49,8	0,1565	4228	1909	144,9	268,2	32,8	76,5	4,41	3,51	1,86	1,88
30	R134a/CO_2	68,9	0,1092	4672	2133	147,9	259,1	42,1	93,7	3,51	2,77	1,45	
	R290/CO_2	67,5	0,1441	3698	2133	279,1	259,1	79,8	93,7	3,50	2,77	1,45	−0,20
	R1270/CO_2	74,7	0,1208	3595	2133	285,1	259,1	83,8	93,7	3,40	2,77	1,43	−1,52
	R600a/CO_2	58,5	0,3609	4523	2133	265,1	259,1	72,2	93,7	3,67	2,77	1,48	2,07
	R1234ze(E)/CO_2	59,8	0,1342	4787	2133	133,7	259,1	36,9	93,7	3,63	2,77	1,47	1,51
40	R134a/CO_2	79,2	0,0943	5213	2377	135,5	249,8	46,0	110,8	2,95	2,25	1,18	
	R290/CO_2	77,7	0,1274	4079	2377	254,9	249,8	87,3	110,8	2,92	2,25	1,18	−0,48
	R1270/CO_2	85,6	0,1070	3960	2377	260,7	249,8	91,7	110,8	2,84	2,25	1,16	−1,73
	R600a/CO_2	67,5	0,3132	5037	2377	245,2	249,8	79,4	110,8	3,09	2,25	1,21	2,22
	R1234ze(E)/CO_2	69,5	0,1156	5348	2377	122,1	249,8	40,4	110,8	3,03	2,25	1,20	1,23

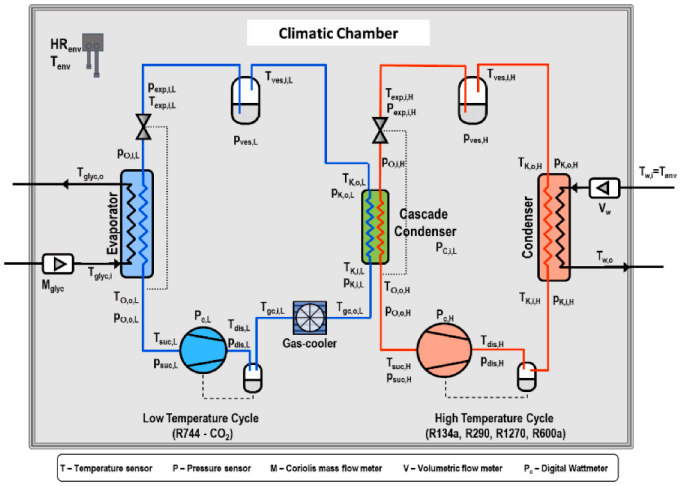

Fig. 3. Experimental cascade plant scheme.

Table 2
Characteristics of the main components.

Component	Main characteristics
Semi hermetic compressor - HTC	Used with R134a BITZER Model: 2HES-1Y-40S. Displacement: 6.5 $m^3 \cdot h^{-1}$ (1.450 rpm) Used with R290 and R1270 DORIN Model H-80CC. Displacement: 4.42 $m^3 \cdot h^{-1}$ (1.450 rpm) Used with R600a and R1234ze(E) BITZER Model: 2EC-2.2Y-40S Displacement:11.4 $m^3 \cdot h^{-1}$ (1.450 rpm) with R600a and 8.78 $m^3 \cdot h^{-1}$ (1.116.5 rpm) with R1234ze(E) Lubricant oil used in all cases: POE SL32
Semi hermetic compressor - LTC	DORIN Model CD150H. Displacement 1.12 $m^3 \cdot h^{-1}$ (1450 rpm) Lubricant Oil: POE C85E.
Oil separator	Used with R134a, R1234ze(E) and R600a - ESK Model: OS-12 Used with R290 and R1270 - Temprite Model 3358 Used with R744 - Temprite Model: 133A
Condenser (HTC)	Insulated brazed plate heat exchanger SWEP Model: B15THx30 plates - Heat transfer area: 0.952 m^2 Secondary fluid: water
Cascade Heat Exchanger (HX_{cc})	Insulated brazed plate heat exchanger SWEP Model: B8THx20 plates - Heat transfer area: 0.414 m^2
Evaporator – LTC	Insulated brazed plate heat exchanger SWEP Model: B15THx20 plates - Heat transfer area: 0.612 m^2
Gas-Cooler – LTC	Cross Flow heat exchanger. ECO. Model LCE-213. Heat transfer area: internal 0.6 m^2, external 3.36 m^2 Electric motor: 75 W
Refrigerant receiver	In HTC Insulated liquid receiver TECNAC. Volume: 5 dm^3 In LTC Insulated High Pressure Vessel. Volume: 20 dm^3
Expansion valve	In HTC - Electronic expansion valve CAREL E2V09 + EVD controller In LTC - Electronic expansion valve CAREL E2V05+ EVD controller Superheat at evaporator outlet set to 7°C in all cases

highest coefficient of performance, on the contrary, R1270 is the refrigerant with the lowest.

- The global coefficient of performance (COP). The highest value is obtained with the refrigerant pair R1234ze(E)/R744 at 20 °C heat rejection temperature, and at 30 °C and 40 °C is the pair R600a/R744 which reaches the highest values. Compared with the pair R134a/R744, the COP values obtained with the four alternative refrigerants are not very different, with 2.22% being the maximum improvement obtained in all simulated cases, and −1,73% the maximum reduction.

Table 3
Characteristics and accuracy of the measurement elements.

Number	Variable	Type	Calibration range	Accuracy
34	Temperature	T-type thermocouple	−40 to 125 °C	± 0.5 °C
4	Pressure	Pressure gauge JOHNSON CONTROLS P499	0 – 30 bar	± 0.08 bar
3	Pressure	Pressure gauge JOHNSON CONTROLS P499	0 – 16 bar	± 0.045 bar
4	Pressure	PMA GmbH Transmitter P30/P31	0 – 50 bar	± 0.15 bar
3	Pressure	PMA GmbH Transmitter P30/P31	0 – 60 bar	± 0.18 bar
1	Pressure	PMA GmbH Transmitter P30/P31	0 to 100 bar	± 0.3 bar
1	Mass flow rate	Coriolis flow meter YOKOGAWA ROTAMASS RCCT34	0 – 0.1 $kg \cdot s^{-1}$	± 0.1% lecture
1	Volumetric flow rate	Magnetic flow meter YOKOGAWA RXF032G	0 – 2.5 $m^3 \cdot h^{-1}$	± 0.25% lecture
2	Electric Power	Digital Wattmeter SENECA K109S	0 – 3.000 W	± 0.5% lecture

3. Experimental facility

3.1. Description

The experimental facility used comprises two single stage vapor compression cycles thermally coupled with a welded plated heat exchanger, called cascade heat exchanger (HX_{cc}). The low temperature cycle (LTC) is charged with R744 in all cases, while the high temperature cycle (HTC) is charged alternatively with R134a, R290, R1270, R600a and R1234ze(E). As heat rejection sink for the HTC condenser, a constant water volumetric flow rate with three inlet temperatures (20°C. 30°C and 40°C) is used. As heat source, a constant water ethylene glycol (50/50 in volume) mass flow rate at an inlet temperature of −20°C is used in all cases. The experimental facility is placed on a climate room, where the same temperature that the one used at the HTC condenser for heat rejection has been maintained. So, both, the gas-cooler mounted at the LTC and the HTC condenser operate at the same heat sink temperature.

The plant scheme and the measurement devices distribution are shown in Fig. 3 Experimental cascade plant scheme. One of the peculiarities of this architecture is the constraint imposed by the refrigerant receivers. Their placement forces no subcooling at the condenser outlet. Thus, whichever modification in the heat transfer rates at both condensers are translated entirely into pressure changes, what means changes in the compressor pressure ratio. The receiver location is the common one in marketed cascade refrigeration plants that are equipped with this type of device. We have charged the refrigerant receiver with 3 kg in all cases. This mass quantity assures that the receiver provides the needed refrigerant mass to the cascade plant according with the operating conditions.

Table 2 summarizes the main characteristics of the components that make up the cascade refrigeration plant, while the characteristics and accuracies of each measurement device are detailed in the Table 3.

Table 4
Average values and standard deviations of heat sink and heat source parameters during tests.

Refrigerant	Heat sink temperature	$T_{climatic\ chamber}$	$T_{w.i}$	$T_{w.o}$	$T_{glyc.i}$	$T_{glyc.o}$	$\dot{m}_{glyc}$	$\dot{V}_w$
	°C	C	° C	° C	° C	°C	$(kg{\cdot}s^{-1})$	$(dm^3{\cdot}s^{-1})$
R134a	20	19.8 ± 0.09	19.9 ± 0.09	26.99±0.07	−20.2 ± 0.30	−24.97±0.32	397.6 ± 1.75	0.266±0.0010
	30	30.3 ± 0.13	30.0 ± 0.09	37.24±0.08	−19.7 ± 0.16	−24.97±0.22	401.4 ± 1.08	0.267±0.0010
	40	39.6 ± 0.13	40.1 ± 0.10	47.39±0.09	−19.8 ± 0.13	−24.97±0.20	404.7 ± 1.16	0.268±0.0008
R290	20	20.3 ± 0.08	19.9 ± 0.09	26.70±0.11	−19.9 ± 0.20	−24.98±0.25	400.1 ± 1.51	0.267±0.0011
	30	30.1 ± 0.12	30.0 ± 0.10	36.79±0.09	−20.1 ± 0.17	−24.78±0.21	402.6 ± 1.55	0.265±0.0009
	40	40.0 ± 0.12	40.0 ± 0.08	47.42±0.10	−20.2 ± 0.17	−24.52±0.22	399.6 ± 1.78	0.263±0.0014
R1270	20	19.9 ± 0.07	20.0 ± 0.11	27.48±0.11	−19.9 ± 0.27	−25.14±0.32	400.2 ± 1.60	0.267±0.0013
	30	30.2 ± 0.10	29.9 ± 0.09	37.54±0.11	−20.0 ± 0.17	−24.78±0.21	403.7 ± 1.39	0.269±0.0010
	40	40.2 ± 0.14	39.9 ± 0.15	47.95±0.12	−20.1 ± 0.12	−24.62±0.15	401.7 ± 1.36	0.267±0.0011
R600a	20	20.6 ± 0.09	20.0 ± 0.11	27.39±0.13	−20.1 ± 0.24	−24.60±0.26	397.9 ± 1.82	0.265±0.0009
	30	30.0 ± 0.11	29.9 ± 0.08	37.12±0.10	−20.0 ± 0.22	−24.50±0.27	398.2 ± 1.74	0.264±0.0008
	40	39.6 ± 0.14	39.7 ± 0.07	46.89±0.11	−20.1 ± 0.11	−24.02±0.18	405.2 ± 0.97	0.266±0.0008
R1234ze(E)	20	19.9 ± 0.11	20.0 ± 0.21	27.36±0.23	−20.0 ± 0.25	−24.72±0.26	402.6 ± 2.00	0.265±0.0011
	30	30.0 ± 0.11	29.9 ± 0.08	37.45±0.10	−20.0 ± 0.22	−24.69±0.27	398.2 ± 1.74	0.264±0.0008
	40	39.6 ± 0.14	39.7 ± 0.07	47.65±0.09	−20.1 ± 0.11	−24.18±0.20	405.2 ± 0.97	0.266±0.0008

We have used different compressors in the HTC to provide the displacement needed with each refrigerant. On the contrary, regarding with the HTC condenser and the HX_{cc}, they have been selected with a heat transfer surface higher enough to accomplish with the heat transfer rate estimated during the plant dimensioning, whichever the refrigerant used. Thus, in the case of the HXcc, the oversizing of the heat transfer surface is 11% for R1270, 9% for R290, 5% for R600a, 3% for R1234ze (E) and 0% for R134a, while in the case of the HTC condenser, the oversizing values are: 108% for R1270, 82% for R290, 74% for R1234ze (E), 73% for R600a and 72% for R134a.

All the information received from the sensors is obtained on-line with two CRio-9074 data acquisition systems from National Instruments. The measurements are gathered by an own developed data application based on Labview, which allows real time analysis, representation, and calculation of the test parameters.

3.2. Test procedure

The heat sink is configured in all tests with a constant volumetric water flow rate to the HTC condenser at a constant inlet temperature. Meanwhile, the heat source is configured in all tests, with a constant water-glycol (50/50 in vol) mass flow rate to the LTC evaporator at a constant inlet temperature. Besides, the indoor climatic chamber temperature is set to the same value that the water inlet temperature to the condenser, thus, the gas cooler placed at the LTC works with the same heat rejection temperature level that the HTC condenser.

Each refrigerant is tested at three heat sink temperatures (20°C. 30°C and 40°C) that simulate a wide range of environmental conditions. A heat source temperature of −20°C is set for all sets. This temperature is the common one in freezing cabinets.

So, since the four refrigerants are tested at the same cooling duty inlet conditions. and due to their great differences in the volumetric cooling capacity, one compressor was used for R134a, another for R600a and R1234ze(E) and another compressor for R290 and R1270. In each case the compressor runs at the proper displacement, as it is shown in Table 2.

The experimental test procedure in all the cases has been equal. Once the system heat sink and heat source parameters (inlet temperature and mass flow rate) are stabilized at the selected operating conditions, data are acquired during 20 min with a frequency of 5 s. The average values of the heat sink and heat source parameters during tests, and their corresponding standard deviations, are summarized at Table 4, to demonstrate the stability of tests.

Table 5
Equations used to calculate the main energy parameters.

$T_{O,L} = \frac{T_{sat.}(p_{O,i,L}) + T_{sat.}(p_{O,o,L})}{2}$	Eq. (20)	$T_{O,H} = \frac{T_{sat.}(p_{O,i,H}) + T_{sat.}(p_{O,o,H})}{2}$	Eq. (21)
$T_{K,L} = \frac{T_{sat.}(p_{K,i,L}) + T_{sat.}(p_{K,o,L})}{2}$	Eq. (22)	$T_{K,H} = \frac{T_{sat.}(p_{K,i,H}) + T_{sat.}(p_{K,o,H})}{2}$	Eq. (23)
$\Delta T_{cc} = T_{K,L} - T_{O,H}$	Eq. (24)	$t = \frac{p_{dis.}}{p_{suct.}}$	Eq. (25)
$q_O = h_{O,o} - h_{O,i}$	Eq. (26)	$w_C = h_{dis.} - h_{suct.}$	Eq. (27)
$\dot{Q}_{glyc} = \dot{m}{\cdot}(c_{p,in}{\cdot}T_{in} - c_{p,out}{\cdot}T_{out})\vert_{glyc}$	Eq. (28)	$\dot{Q}_w = \dot{V}{\cdot}\rho{\cdot}c_p{\cdot}(T_{out} - T_{in})\vert_w$	Eq. (29)
$\dot{m}_{ref,L} = \frac{(h_{O,o,L} - h_{O,i,L})}{\dot{Q}_{glyc}}$	Eq. (30)	$\dot{m}_{ref,H} = \frac{(h_{K,o,H} - h_{K,i,H})}{\dot{Q}_w}$	Eq. (31)
$\dot{Q}_{K,L} = \dot{m}_{ref,L}{\cdot}(h_{K,o,L} - h_{K,i,L})$	Eq. (32)	$\dot{Q}_{O,H} = \dot{m}_{ref,H}{\cdot}(h_{O,o,H} - h_{O,i,H})$	Eq. (33)
$\eta_{G,L} = \frac{\dot{m}_{ref,L}{\cdot}(h_{dis,L} - h_{suct,L})}{P_{c,L}}$	Eq. (34)	$\eta_{G,H} = \frac{\dot{m}_{ref,H}{\cdot}(h_{dis,H} - h_{suct,H})}{P_{c,H}}$	Eq. (35)
$COP_L = \frac{\dot{Q}_{O,L}}{P_{c,L}}$	Eq. (36)	$COP_H = \frac{\dot{Q}_{O,H}}{P_{c,H}}$	Eq. (37)
$COP = \frac{\dot{Q}_{O,L}}{P_{c,L} + P_{c,H}}$			Eq. (38)

3.3. Data reduction

The set of equations used to calculate the energy parameters involved in the analysis are shown in Table 5. All refrigerants and water properties from direct measured variables are evaluated using Refprop v.10 (Lemmon et al., 2018), while properties of the water-glycol mixture are evaluated using SecCool v1.33 [(IPU 2007)]

Each enthalpy is calculated at its respective pressure and temperature, except the enthalpy at evaporator inlet, which is equal to the enthalpy at the expansion valve inlet. For the calculation of the phase change temperatures in each cycle, the criteria given by (ASERCOM 2015) have been adopted. Therefore, they are calculated as the arithmetic mean between the inlet and outlet saturation temperatures in each heat exchanger, see Eqs. (19) – 23. The phase change temperature difference in the cascade heat exchanger is calculated with equation 24. The compressor pressure ratio (t), the specific cooling capacity (q_o) and the specific compression work (w_c), whatever the cycle, are evaluated using equations 25, 26 and 27, respectively. The heat transfer rate from water-glycol to the refrigerant in the LTC evaporator, and from refrigerant to water in the HTC condenser, are calculated with equations 28 and 29, respectively. The refrigerant mass flow rates in HTC and LTC are obtained from energy balances in the HTC condenser and the LTC evaporator, respectively, using equations 30 and 31. Heat transfer rates

Table 6
Measured parameters of thermodynamic cycles.

		Test	$T_K \pm \delta$ (°C)	$T_O \pm \delta$ (°C)	$T_{suct} \pm \delta$ (°C)	$T_{disch} \pm \delta$ (°C)	$v_{suct} \pm \delta$ (m3·kg-1)	$q_O \pm \delta$ (kJ·kg-1)	$w_C \pm \delta$ (kJ·kg-1)	$t \pm \delta$ (-)	$\dot{m}_{ref} \pm \delta$(Kg·h-1)	$\eta_G \pm \delta$ (-)
R134a /R744	HTC	20	26.8	−14.6	−1.2	70.3	0.127	165.6	55.4	4.3	37.54	0.48
			±0.51	±0.61	±0.60	±0.53	±0.09	±0.95	±0.82	±0.22	±1.89	±0.05
		30	36.8	−12.1	2.9	81.8	0.117	153.1	60.9	5.2	39.56	0.52
			±0.51	±0.61	±0.52	±0.51	±0.08	±0.88	±0.80	±0.24	±1.95	±0.05
		40	46.8	−9.2	6.3	92.8	0.106	138.2	66.3	6.1	41.64	0.54
			±0.52	±0.61	±0.52	±0.53	±0.08	±1.06	±0.82	±0.26	±2.03	±0.05
	LTC	20	−9.1	−29.1	−16.7	80.4	0.029	266.0	85.4	1.9	19.91	0.25
			±0.51	±0.56	±0.61	±0.64	±0.02	±8.75	±0.91	±0.02	±0.68	±0.04
		30	−5.8	−28.4	−14.3	95.7	0.029	257.6	97.3	2.0	19.59	0.26
			±0.50	±0.53	±0.52	±0.69	±0.01	±0.96	±0.87	±0.02	±0.14	±0.03
		40	−2.0	−27.9	−12.9	106.7	0.028	248.2	105.7	2.2	19.26	0.27
			±0.51	±0.54	±0.52	±0.61	±0.01	±0.97	±0.86	±0.02	±0.15	±0.03
R290 /R744	HTC	20	26.4	−15.8	−0.4	70.9	0.171	314.2	109.6	3.5	18.51	0.43
			±0.52	±0.80	±0.56	±0.51	±0.06	±1.56	±1.14	±0.13	±0.97	±0.04
		30	36.3	−13.2	2.6	81.8	0.169	290.1	120.7	4.4	19.06	0.48
			±0.53	±0.80	±0.53	±0.52	±0.05	±10.02	±0.98	±0.13	±1.00	±0.04
		40	46.7	−8.6	8.3	92.7	0.157	266.6	127.5	5.1	21.14	0.53
			±0.53	±0.80	±0.64	±0.52	±0.05	±13.97	±1.18	±0.13	±1.03	±0.04
	LTC	20	−9.9	−30.6	−16.2	85.2	0.031	268.1	88.8	2.0	21.29	0.25
			±0.50	±0.56	±0.55	±0.56	±0.02	±1.07	±0.85	±0.02	±0.20	±0.03
		30	−5.8	−30.0	−13.6	100.1	0.031	258.6	99.9	2.1	20.22	0.26
			±0.51	±0.69	±0.58	±0.64	±0.02	±1.23	±0.93	±0.04	±0.20	±0.03
		40	−1.3	−28.4	−11.5	110.4	0.029	246.9	107.3	2.3	19.33	0.28
			±0.51	±0.55	±0.54	±0.63	±0.01	±1.04	±0.87	±0.02	±0.20	±0.03
R1270 /R744	HTC	20	26.6	−18.0	−4.3	77.3	0.152	316.5	115.5	3.7	20.20	0.45
			±0.53	±0.66	±0.53	±0.51	±0.05	±1.51	±1.36	±0.23	±0.97	±0.04
		30	36.5	−15.1	0.2	90.4	0.139	298.3	128.0	4.3	20.88	0.47
			±0.54	±0.66	±0.53	±0.52	±0.05	±10.11	±1.14	±0.13	±0.97	±0.04
		40	47.1	−12.1	5.3	104.7	0.128	276.0	141.9	4.9	21.44	0.48
			±0.56	±0.66	±0.52	±0.51	±0.04	±10.04	±1.11	±0.13	±0.99	±0.04
	LTC	20	−12.1	−30.1	−16.4	76.9	0.031	273.4	82.2	1.8	21.36	0.24
			±0.50	±0.57	±0.56	±0.58	±0.02	±8.78	±0.87	±0.02	±0.71	±0.04
		30	−8.0	−29.1	−14.6	91.5	0.029	263.4	94.0	1.9	20.52	0.25
			±0.51	±0.55	±0.58	±0.61	±0.01	±1.04	±0.88	±0.02	±0.18	±0.03
		40	−3.7	−28.5	−12.4	104.6	0.029	252.9	103.4	2.2	20.25	0.27
			±0.51	±0.57	±0.58	±0.58	±0.02	±1.11	±0.87	±0.02	±0.18	±0.03
R600a /R744	HTC	20	27.9	−12.8	0.1	66.1	0.401	300.9	105.1	4.3	20.43	0.42
			±0.52	±0.63	±0.58	±0.51	±0.16	±1.24	±1.13	±0.38	±1.02	±0.04
		30	38.1	−10.3	4.3	75.3	0.369	288.8	113.1	5.1	20.82	0.46
			±0.51	±0.63	±0.63	±0.51	±0.14	±1.23	±1.15	±0.41	±1.02	±0.04
		40	47.1	−7.4	9.3	85.5	0.351	260.7	122.4	6.0	21.66	0.49
			±0.51	±0.63	±0.55	±0.51	±0.14	±1.43	±1.13	±0.45	±1.07	±0.04
	LTC	20	−7.6	−28.7	−16.5	84.2	0.029	262.9	88.7	5.2	19.56	0.26
			±0.51	±0.55	±0.75	±0.61	±0.02	±8.75	±0.93	±0.02	±0.68	±0.04
		30	−4.7	−28.0	−15.1	94.6	0.028	255.6	96.7	2.1	19.51	0.27
			±0.51	±0.56	±0.56	±0.70	±0.01	±1.01	±0.91	±0.02	±0.20	±0.03
		40	−0.6	−27.5	−12.8	108.9	0.028	244.9	107.4	2.3	18.35	0.28
			±0.51	±0.53	±0.54	±0.64	±0.01	±0.99	±0.87	±0.02	±0.13	±0.03
R1234ze(E) / R744	HTC	20	28.0	−13.7	−1.5	63.8	0.154	150.5	52.6	4.6	42.20	0.44
			±0.58	±0.57	±0.53	±0.54	±0.12	±0.99	±0.82	±0.31	±2.17	±0.04
		30	37.9	−11.1	1.9	75.9	0.140	137.8	59.6	5.4	43.87	0.46
			±0.52	±0.57	±0.53	±0.52	±0.11	±0.99	±0.81	±0.33	±2.10	±0.04
		40	48.1	−8.4	5.3	87.2	0.128	124.5	65.6	6.4	45.84	0.47
			±0.52	±0.57	±0.53	±0.51	±0.10	±1.11	±0.92	±0.43	±2.15	±0.04
	LTC	20	−8.3	−28.7	−16.7	81.6	0.029	264.0	86.5	1.9	20.24	0.26
			±0.51	±0.53	±0.56	±0.53	±0.01	±1.02	±0.84	±0.02	±0.23	±0.03
		30	−5.4	−28.0	−14.8	94.2	0.028	256.7	96.3	2.0	19.41	0.26
			±0.50	±0.52	±0.53	±0.59	±0.01	±0.95	±0.84	±0.02	±0.13	±0.03
		40	−1.4	−27.3	−12.5	108.3	0.028	246.6	107.2	2.2	19.15	0.26
			±0.50	±0.51	±0.52	±0.53	±0.01	±0.93	±0.81	±0.02	±0.11	±0.03

in cascade heat exchanger are obtained with equations 32 and 33. The compressor global efficiencies in both cycles are evaluated with equations 34 and 35. Finally, the corresponding coefficients of performance of each cycle are calculated with equations 36 and 37, and the overall coefficient of performance of the cascade refrigeration plant with equation 38.

3.4. Data uncertainty treatment

According to (JCGM, 2008), the uncertainty of directly measured parameters (u_D), such as pressure, temperature, relative humidity, electrical consumption volumetric and mass flow rates, has been estimated considering the standard deviation (u_σ). and the accuracy of the measurement (u_M) devices. The first one is obtained from measured data, and the second one, from that provided by device manufacturers. It has been supposed a Gaussian distribution for the uncertainties with a 95% level of confidence, so the expression used to calculate u_D is that proposed in (Coleman and Steele, 2018). shown in Eq. (39).

$$u_D = t_{95} \cdot \sqrt{u_M{}^2 + u_\sigma{}^2} \approx 2 \cdot \sqrt{u_M{}^2 + u_\sigma{}^2} \quad (39)$$

Table 7
Main energy parameters and efficiencies.

Refrigerant	TEST	$\Delta T_{lm,CCk}$ °C±δ(°C)	$\Delta T_{lm,Hk}$ C±δ(°C)	Q_{oL} kW±δ(kW)	Q_{cc} kW±δ(kW)	$P_{c.HTC}$ kW±δ(kW)	$P_{c.LTC}$ kW±δ(kW)	COP_{HTC} -±δ(-)	COP_{LTC} -±δ(-)	$COP_{Overall}$ -±δ(-)
R134a	20	5.78±0.79	3,28±0.76	1.471±0.014	1.726±0.087	0.699±0.016	0.626±0.023	2.47±0.022	2.35±0.017	1.11±0.026
	30	6.88±0.50	3,11±0.49	1.402±0.009	1.682±0.084	0.786±0.015	0.659±0.024	2.14±0.017	2.13±0.012	0.97±0.020
	40	8.04±0.51	3,20±0.60	1.328±0.009	1.598±0.079	0.879±0.018	0.686±0.024	1.82±.0140	1.93±0.011	0.85±0.017
R290	20	6.21±0.94	3,02±0.82	1.586±0.013	1.616±0.085	0.762±0.013	0.615±0.022	2.12±0.021	2.58±0.015	1.15±0.024
	30	7.96±0.51	3,04±0.64	1.452±0.012	1.536±0.096	0.835±0.014	0.654±0.024	1.84±0.018	2.22±0.012	0.98±0.020
	40	7.89±0.51	3,37±0.45	1.326±0.013	1.565±0.112	0.947±0.014	0.690±0.027	1.65±0.015	1.92±0.010	0.81±0.017
R1270	20	6.44±0.83	2,68±0.77	1.623±0.014	1.776±0.085	0.858±0.020	0.598±0.022	2.07±0.020	2.72±0.018	1.12±0.025
	30	7.58±0.51	2,77±0.62	1.501±0.012	1.730±0.099	0.953±0.014	0.646±0.025	1.82±0.016	2.33±0.011	0.94±0.018
	40	9.24±0.51	3,53±0.57	1.423±0.011	1.644±0.096	1.063±0.015	0.657±0.025	1.55±0.013	2.16±0.010	0.83±0.015
R600a	20	5.64±0.81	3,97±0.78	1.428±0.015	1.708±0.085	0.784±0.019	0.656±0.029	2.189±0.023	2.18±0.017	0.99±0.026
	30	6.16±0.51	4,33±0.55	1.385±0.013	1.670±0.082	0.830±0.012	0.663±0.024	2.01±0.017	2.09±0.012	0.93±0.019
	40	7.54±0.51	3,82±0.58	1.249±0.007	1.569±0.078	0.899±0.014	0.690±0.024	1.75±0.013	1.81±0.008	0.79±0.014
R1234ze(E)	20	5.82±0.76	4,26±0.70	1.484±0.016	1.765±0.091	0.800±0.018	0.640±0.027	2.20±0.022	2.32±0.017	1.03±0.026
	30	6.29±0.50	4,36±0.65	1.384±0.008	1.679±0.081	0.900±0.017	0.661±0.026	1.86±0.016	2.09±0.011	0.89±0.018
	40	7.83±0.50	4,49±0.52	1.312±0.006	1.586±0.076	1.006±0.016	0.683±0.023	1.58±0.011	1.92±0.008	0.78±0.013

Being t_{95} the distribution factor of the uncertainty with a 95% level of confidence which is approximated to 2.

The uncertainty related to thermodynamic properties (u_{TH}), like enthalpy or specific volume, is calculated using the methodology explained by (Moffat, 1985). Eqs. (40) – (43) synthetize this methodology.

$$prop_{TH} = f(x.y) \tag{40}$$

$$u_{TH.x} = \frac{|prop_{TH}(x - u_{D.x}.y) - prop_{TH}(x.y)| + |prop_{TH}(x + u_{D.x}.y) - prop_{TH}(x.y)|}{2} \tag{41}$$

$$u_{TH.y} = \frac{|prop_{TH}(x.y - u_{D.y}) - prop_{TH}(x.y)| + |prop_{TH}(x.y + u_{D.y}) - prop_{TH}(x.y)|}{2} \tag{42}$$

$$u_{TH} = \sqrt{u_{TH.x}^2 + u_{TH.y}^2} \tag{43}$$

Where:

- $prop_{TH}$ is the thermal property, function of the directly measured parameters x and y
- $u_{TH.x}$ is the partial uncertainty of the thermal property as function of the parameter x
- u_{THy} is the partial uncertainty of the thermal property as function of the parameter y
- u_{TH} is the uncertainty related to the thermal property

For the uncertainties of indirect parameters (ε_I), like cooling capacity or energy efficiency (COP), the error propagation from directly measured parameters is considered. They are evaluated using the criteria exposed by [Moffat-2018]. The expression used is shown in Eq. (44).

$$I = F(X_1.X_2 \ldots X_N)$$

$$\varepsilon_I = \sqrt{\sum_i^N \left(\left(\frac{\partial F}{\partial X_i}\right)^2 \cdot \varepsilon_i^2\right)} \tag{44}$$

Where:

- I it is the indirect parameter and F is the function to calculate it.
- e_i is the uncertainty related to the directly measured parameters or the thermodynamic properties
- X_i are the variables used in function F
- N is the number of variables of the function F

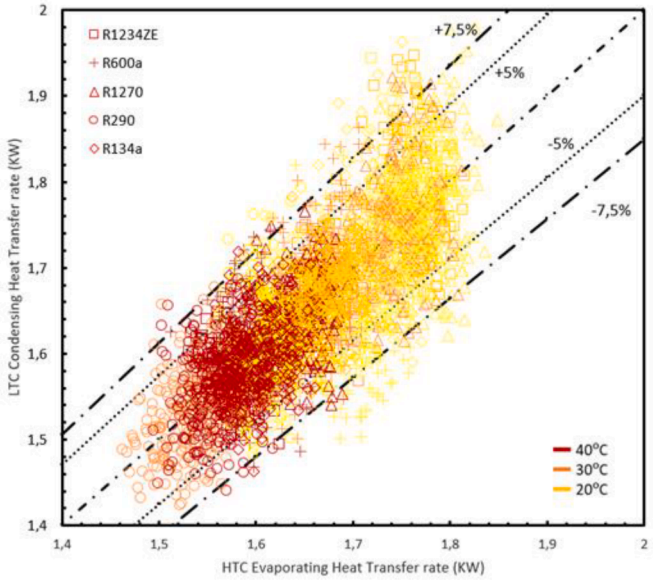

Fig. 4. Energy balance at the cascade heat exchanger.

Accordingly, the uncertainties calculated are shown in Tables 6 and 7, in addition to the graphs presented in Section 4.

3.5. Data validation

The confidence in the measured data is evidenced in Fig. 4, where the

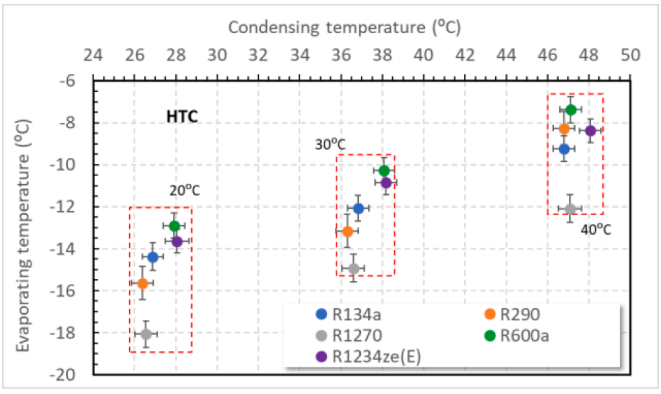

Fig. 5. HTC phase change temperatures.

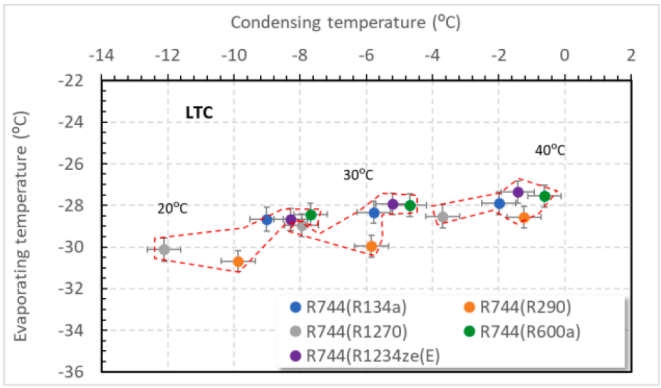

Fig. 6. LTC phase change temperatures.

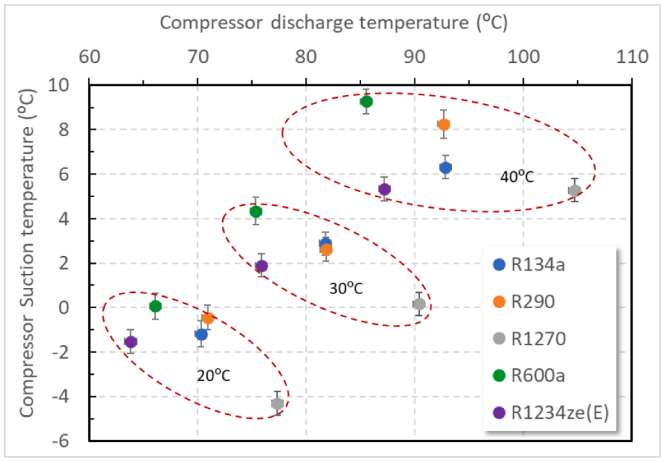

Fig. 7. Compressor suction and discharge temperatures in HTC.

calculated heat transfer rates on the HTC and LTC sides are confronted at the cascade heat exchanger. That is, the HTC cooling duty is represented against the LTC rejection capacity, showing a majority discrepancy into ±5%.

4. Analysis of results

The main parameters describing both vapor compression cycles, obtained for each refrigerant pair and each heat rejection temperature, are collected in Table 6.

As per the phase change temperatures their evolutions are presented in Figs. 5 and 6 for greater clarity. Both cycles shown an increase in evaporating and condensing temperatures as the heat sink temperature increases, however, this trend is more pronounced in the HTC. Regarding the HTC condensing temperatures, R600a and R1234ze(E) present the highest ones. Considering that the heat sink temperature is almost the same for all refrigerants (if we discard the standard deviations), the higher values could be considered as a worse heat transfer behavior of R600a and R1234ze(E) respect the rest ones in the condenser side. The difference between the refrigerants condensing temperatures, at each heat sink temperatures, varies from around 2°C to around 1°C when T_{win} raises from 20°C to 40°C, this is indicative that the condenser is adequately sized.

Regarding the HTC evaporating temperatures, R1270 generates the lowest while R600a and R1234ze(E) the highest, with the amplitude of variation stable at the three heat rejection temperatures (6°C). R290 shows the major evaporating temperature slope with the T_{win} increase, followed by R600a.

In the LTC the evaporating temperature of R744 presents lower variations. The highest values are those obtained when it is working paired with R600a or R1234ze(E). and the lowest when paired with R290. The maximum difference is 2.5 ºC. About the condensing temperatures in LTC, R744 also presents higher values when paired with R600a, and lower when paired with R1270. The maximum difference is around 4ºC with the three heat sink temperatures tested.

The higher evaporating temperatures generated with the R600a and the R1234ze(E) in the HTC, force higher condensing temperatures in the LTC than those obtained with the rest of refrigerants. This penalizes the LTC, because the compression ratio increases more than necessary in this cycle, forcing a larger compressor electrical consumption. In addition, it the vapor quality at the LTC evaporator inlet increases, thus worsening the evaporation process.

It seems that R600a and R1234ze(E) are not able of absorbing the cooling duty of the LTC in the cascade condenser and tend to evaporate at higher temperatures than the others, probably due to their specific volume, which is higher than the rest of refrigerants tested, or because of they have worse heat transfer properties, or a combination of both reasons. So, in any case, R1234ze(E) and R600a need to rise the evaporating temperature to increase their mass flow rates, thus counteracting this deficiency, however, there is a counterpart, which is the reduction in the R744 mass flow rate (see penultimate column of Table 6).

It is worth mentioning at this point an aspect that differentiates the measured results from those obtained with the theoretical model. This is that in the theoretical model we have considered that the LTC behavior is not influenced by the refrigerant charged in the HTC, but we have verified from measured data that the behavior of the LTC is influenced by that of the HTC one, this is the main source of the discrepancy between the theoretical model and the experimental results.

Apart from pressure losses, the phase change temperatures are the main parameter affecting the compression ratio. Thus, from Fig. 6 and data from Table 6,. it can be justified that LTC compressor works with the lowest compression ratio when the HTC is charged with R1270, since it presents the minimum condensing temperature. Conversely, it works with the highest compression ratio when HTC is charged with R290, since the evaporating temperature obtained in the LTC is the lowest respect the obtained with the other refrigerants. The refrigerants R600a, R1234ze(E) and R134a generate very similar compression ratios in the LTC.

In the HTC. the analysis of pressure ratio could not be made in base phase change temperatures. because each refrigerant has its own p-V-T behavior. So, what is directly appreciated in Table 6 is that R1234ze(E) generates the highest compression ratios of the whole refrigerants set. Also, we can observe the similarity between compression ratios produced by R600a and R134a. and those between R1270 and R290, being the first ones higher than the last ones, but all of them present the same trend with the heat rejection temperature. The trends in the experimental compression ratios between refrigerants are in accordance with those obtained with the theoretical model (see Table 1)

The compressor global efficiencies in the HTC are calculated using eq. 35. Although three different compressors have been used, the global efficiencies are very similar, being 6% the maximum difference at each heat sink temperature. The highest values are calculated for R134a compressor (51.3% in average). and the minimum for R600a compressor (45.7% in average). In the LTC has been used the same compressor in all tests with 26.2% of average global efficiency. The reduced value in the R744 compressor could be due to the compressor is prepared for operating at supercritical conditions, not for subcritical ones. All the compressors show a linear increase trend in their global efficiencies with the compression ratio increase, but their measured global efficiencies are lower than those considered in the theoretical model (0,6 for those used in the HTC and 0,3 for the one used in the LTC)

The refrigerant mass flow rates in the HTC, gathered in Table 6, reveal that with respect R134a, the R290, the R1270 and the R600a use a −50.6%, a −46.9% and a −47–3% on average. Meanwhile the mass flow rate moved with R1234ze(E) is 11.1% higher than with R134a.

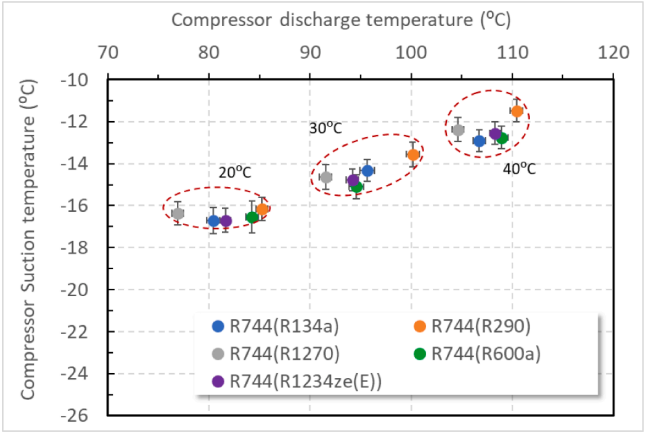

Fig. 8. Compressor suction and discharge temperatures in LTC.

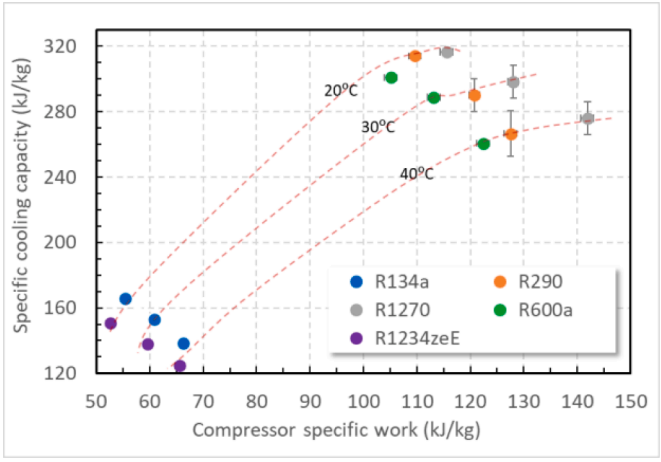

Fig. 9. Specific compression work and cooling capacity at HTC.

Respect to the suction and discharge temperatures associated with the HTC compressor, Fig. 7 shows that there is a great difference in discharge temperatures between refrigerants, but in suction temperatures the difference is much lower. Thus, while the discharge temperature amplitude reaches 13 °C, 15 °C and 19 °C, at heat sink temperatures of 20 °C, 30 °C and 40 °C, respectively, the suction temperature amplitude is around 4 °C in all cases. The difference in discharge temperature becomes greater as the heat sink temperature increases. The R1270 presents the hottest discharge temperature values, followed by the R134a and the R290 with very similar values, and finally, the least hot discharge temperature is obtained with the R600a and with the R1234ze(E), once again, with very similar values between them. This structure is the same that the one obtained with the theoretical model. In any case not extremely values are reached when using whichever four refrigerants. Regarding the suction temperature, the minimum ones are obtained with the R1270 and the maximum ones with the R600a. Notwithstanding, the differences are very low, around 4 °C.

In Fig. 8, the LTC compressor suction and discharge temperatures are depicted. The suction temperature values at each heat sink temperature tested are similar, whichever the refrigerant paired with R744. The discharge temperature shows discrepancies around 10°C, being the hottest values obtained those measured when R290 is paired with R744, and the least hot when R1270 is the refrigerant paired. Due to the high temperature values obtained at the compressor discharge in the LTC, a gas-cooler is needed at the discharge line, to avoid extremely thermal stress at the cascade heat exchanger.

Specific cooling capacities and compression works are illustrated in

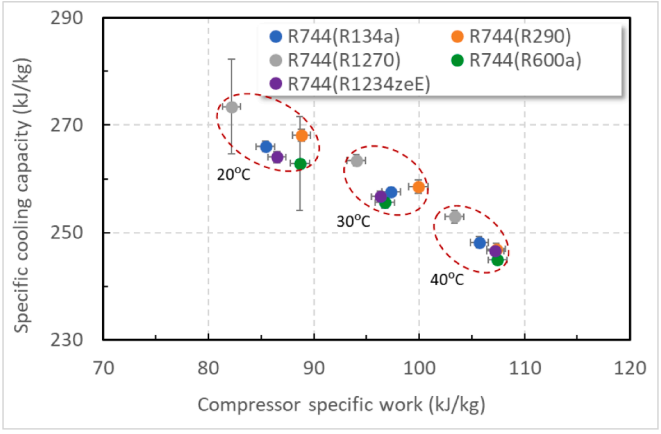

Fig. 10. Specific compression work and cooling capacity at LTC.

Figs. 9 and 10. In general, qo and wc has opposite trends with the heat sink temperature increase, lowering in the first case, and increasing in the second.

In Fig. 9, it is observed that hydrocarbons present about two times greater compressor specific work values and specific cooling capacities, than HFCs and HFOs tested. The R1234ze(E) presents the lowest values at each heat rejection level, and R1270 the highest. Compared to R134a, the three hydrocarbons, R290, R1270 and R600a, have average increases of 90.7%, 95.3% and 87.6%, respectively, in q_o. Likewise, they present average increases of 96.1%, 110.9% and 86.3%, respectively, in w_c. The q_o and w_c, in the case of R1234ze(E) are respectively 9.6% and 2.7% lower than those ones measured with R134a. The trends obtained in the experimental data are qualitatively the same as in the theoretical model. However, the values measured in the tests are higher than the theoretical ones, being this discrepancy greater the higher the heat sink temperature.

In the LTC, see Fig. 10,we measure the highest qo and the lowest wc values when R744 is paired with R1270. R600a paired with R744 results in the lower qo values at the LTC, but not much lower than those measured with the rest of pairings. The same occurs with the wc. These variations do not appear in the theoretical model, and their influence in the HTC, neither. They are due to the heat transfer behavior in the HXcc and are in the basis of discrepancies between experimental and theoretical results.

The Table 7 gathers the calculated main energy parameters in the different test conditions. The logarithmic mean temperature differences in the cascade heat exchanger ($\triangle T_{lm,CCk}$) and in the HTC condenser ($\triangle T_{lm,Hk}$) increase with the heat sink temperature. R600a and R1234ze (E) present the highest values of $\triangle T_{lm,Hk}$ and the lowest values of $\triangle T_{lm,CCk}$ which is in agreement their phase change temperatures in the HTC. On the contrary, R290 and R1270 generate the lowest values of $\triangle T_{lm,Hk}$ and the highest value of $\triangle T_{lm,CCk}$, especially at 20 °C and 30 °C of heat sink temperature. It should be noted that comparing phase change temperatures and $\triangle T_{lm}$, the lowest values of $\triangle T_{lm,CCk}$ achieved with R600a and R1234ze(E), are obtained with high T_{oH} and T_{kL}, while the higher values achieved with R290 and R1270 are obtained with low T_{oH} and T_{kL}. Accordingly with this fact and the COP results obtained, it should be stated that to get better COP results it is more important keep low values of T_{kL} than to achieve low values of $\triangle T_{lmccK}$, if that means high T_{kL}. It is evident that refrigerants evaporating at higher temperatures in the HTC, produces higher condensing and evaporating temperatures in the LTC. This fact penalizes the LTC, because reduces its cooling capacity and increases its compressor specific work.

It is common to all refrigerants the decrease in $\dot{Q}_{O,L}$, and the increase in $P_{c,LTC}$ and $P_{c,HTC}$ with the increase in heat sink temperature. In particular, with respect to the values obtained with the refrigerant pair R134a/R744, the pair R1270/R744 improves the cooling capacity of the

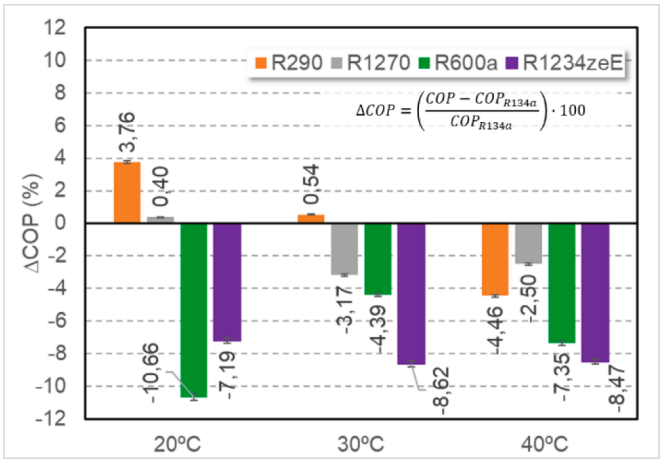

Fig. 11. Relative COP variation respect to R134a.

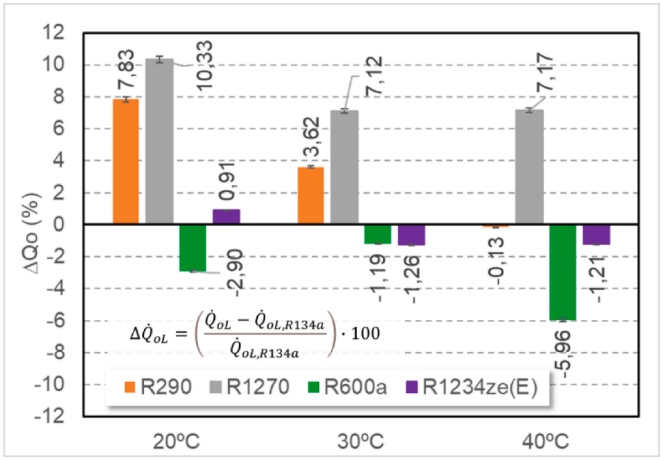

Fig. 12. Relative $\dot{Q}_{O.L}$ variation respect to R134a.

plant ($\dot{Q}_{O.L}$) by a 10% at 20 °C to a 7% at 40 °C of heat sink temperature, as is shown in Fig. 12, while reduces between 2% to 4.5% the electric energy consumption of the LTC compressor in all the operating conditions tested. In contrast, the HTC compressor increases the electric power around 21%. The combination of the values of these parameters makes the overall COP of the plant to be slightly minor, about −2% at 30 °C and 40 °C (see Fig. 11). R290 paired with R744 allows better cooling capacities of the cascade refrigeration plant at 20°C, but this improvement is reduced as the heat sink temperature increases. So, no cooling capacity improvement is registered when the heat rejection temperature is 40°C (see Fig. 12). The overall COP obtained with the pair R290/R744 respect to the pair R134a/R744, ranges from 3.8% at 20°C of heat sink temperature to −4.4% at 40 °C of heat sink temperature. Comparing the results of the pair R600a/R744 against the pair R134a/R744. in the whole operating range tested, no improvement is found in the Q_{oL} (a reduction up to 6% is obtained at 40°C), and neither in the COP, where a maximum reduction of −8% is achieved (see Figs. 11 and 12). As in the previous pair, the pair R1234ze(E)/R744 neither generates energy improvements respect to the R134a/R744 pair, with reductions in COP ranging from 8% to 4%, and neglecting variations in cooling capacity in the LTC.

Regarding the parameters in $\dot{Q}_{O.L}$, $P_{c,LTC}$ and Pc,HTC, there is neither quantitative nor qualitative coincidence between the experimental and the theoretical results. The heat transfer and thermodynamical properties are at the background of those discrepancies because it results in different phase change pressures and refrigerant mass flow rates, that affect the electrical power consumption in the compression and the heat transfer rates in the heat exchangers.

Considering the oversizing values of the heat transfer surface for each refrigerant given in Section 3.1, it is probable that with further oversizing of the HXcc, energy results would have improved for R600a and R1234ze(E), since it could be a factor influencing the results, but not the main one, because from the experimental results, no clear correlation is observed between the oversizing values and the energy results. For instance, R134a gets better performance than R600a with the lowest oversizing values.

5. Environmental analisy. TEWI

Environmental concerns drive the development of different parameters to evaluate the environmental impact. At the refrigeration field, Total Equivalent Warming Impact (TEWI) is one of the most recognized. It was devised at the 1990s to combine the global warming effects corresponding to the carbon dioxide released due to the energy consumption (indirect effect) and the refrigerant emissions (direct effect) during the system lifetime. Eq. (45) is used to evaluate the calculation of the TEWI.

$$TEWI = \left(GWPR_{efHTC} + GWOR_{efLTC}\right)LN + \left[GWP_{RefHTC}\, m_{RefHTC}\left(1-\alpha_{RefHTC}\right)\right] + \left(GWP_{RefLTC}\, LN\right) + \left[GWP_{RefLTC}\, m_{RefLTC}\left(1-\alpha_{RefLTC}\right)\right] + \left(E_{Year}\, \beta N\right) \quad (45)$$

Where:

- GWP_{RefHTC}: is the global warming impact of the refrigerant charged at the High Temperature cycle over 100 years
- GWP_{RefLTC}: is the global warming impact of the refrigerant charged at the Low Temperature cycle over 100 years
- L: annual leakage rate of the cascade plant. Considered 15% according to (EPA 2016) EPA-2016.
- N: the cascade plant lifespans. Assumed 15 years according to (Morlet and Dupont, 2017).
- m_{RefHTC}: High temperature cycle refrigerant mass charge (3.5 kg).
- m_{RefLTC}: Low temperature cycle refrigerant mass charge (5.5 kg).
- α_{RefHTC}: Recovery/Recycling factor in the High Temperature cycle. Assumed 15% according to Morlet et al. 2017.
- α_{RefLTC}: Recovery/Recycling factor in the Low Temperature cycle. Assumed 15% according to Morlet et al. 2017.
- β: carbon dioxide equivalent emissions factor per electric energy generated (CO_{2eq}./kWh_e). Considered 0.14 $kgCO_{2eq}/kWh_e$ in Spain in year 2021, according with Red Electrica Group data, the electricity market technical supervisor (https://www.ree.es/es/datos/generacion/no-renovables-detalle-emisiones-CO2)
- E_{year}: Annual Average Electric Energy demand

The GWP values have been obtained from the IPCC's 5th Assesment Report (IPCC/TEAP 2015). being GWP_{100} = 1.430 in the case of R134a, GWP_{100} = 3 in the case of R290, GWP_{100} = 2 in the case of R1270, GWP_{100}= 3 in the case of R600a, GWP_{100}=7 in the case of R1234ze(E), and finally GWP_{100}=1 in the case of CO_2

Finally, the parameter "E_{year}", has been calculated assuming that the installation has 100% of the cooling demand during a timetable from 7:00 to 22:00 and that it has 50% of its cooling demand between 22:00 and 7:00. This schedule would correspond to the opening and closing hours of stores and supermarkets in accordance with Iyer et al. (2015) and Funder-Kristensen et al. (2017). This assumption implies that the power consumed by the installation is reduced by 50% during closing hours.

To simulate the heat rejection conditions the hourly average dry bulb temperature profile of three Spanish cities as are Bilbao, Valencia and Seville, obtained from (DOE. U.S. Department of Energy 2022) software, it has been considered. These locations present different climate

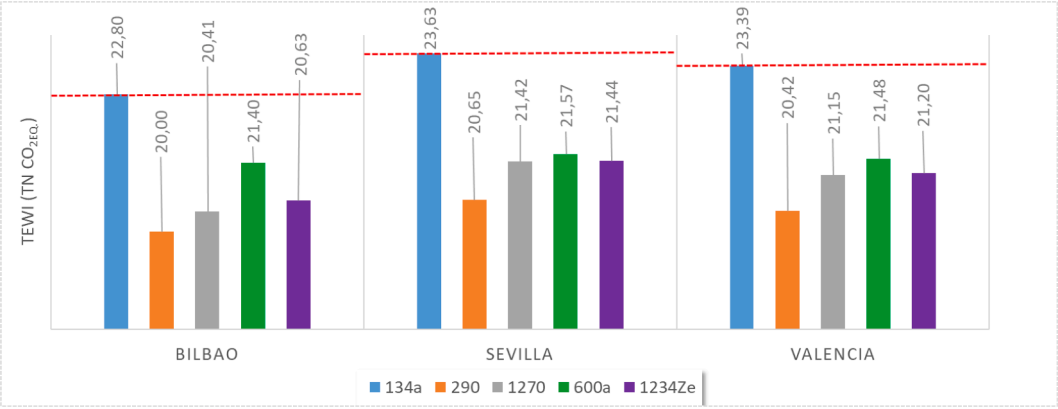

Fig. 13. TEWI values for three Spanish cities.

Table 8
Direct and indirect values of TEWI.

Location	Refrigerant	$TEWI_{Direct}$ Tn CO_{2eq}	$TEWI_{Indirect}$ Tn CO_{2eq}	$TEWI_{Total}$ Tn CO_{2eq}	Relative Direct to Total (%)	Indirect to Total (%)	$\frac{TEWI_{Ref} - TEWI_{R134a}}{TEWI_{R134a}} \cdot 100$
Bilbao	R134a	3.95	18.85	22.80	17.34	82.66	0.00
	R290	0.02	19.98	20.00	0.08	99.92	−12.30
	R1270	0.01	20.39	20.41	0.07	99.93	−10.51
	R600a	0.02	21.39	21.40	0.07	99.93	−6.14
	R1234ze(E)	0.03	20.60	20.63	0.13	99.87	−9.52
Seville	R134a	3.95	19.68	23.63	16.73	83.27	0.00
	R290	0.02	20.63	20.65	0.08	99.92	−12.64
	R1270	0.01	21.41	21.42	0.06	99.94	−9.34
	R600a	0.02	21.56	21.57	0.07	99.93	−8.72
	R1234ze(E)	0.03	21.41	21.44	0.13	99.87	−9.27
Valencia	R134a	3.95	19.43	23.39	16.91	83.09	0.00
	R290	0.02	20.41	20.42	0.08	99.92	−12.68
	R1270	0.01	21.14	21.15	0.06	99.94	−9.57
	R600a	0.02	21.47	21.48	0.07	99.93	−8.14
	R1234ze(E)	0.03	21.17	21.20	0.13	99.87	−9.37

conditions, which represent the Spanish weather. In addition, a polynomial adjustment to find out the installation's electrical consumption based on the ambient temperature and the experimental data is made.

Consequently, the TEWI values obtained are shown in Fig. 13. All the alternative refrigerants tested, show reductions of the CO2 equivalent emissions. R290 is the refrigerant with greater reductions. The detailed values of direct and indirect TEWI, besides the relative variation respect to R134a, are gathered at Table 8.

6. Conclusions

In conclusion, four low-GWP refrigerants have been tested, the three commonly used hydrocarbons R600a, R1270 and R290, and the HFO-1234ze(E), against the R134a, all of them paired with R744 in a cascade refrigeration plant. Tests have been developed in a wide range of heat sink temperatures (20ºC to 40ºC) and −20ºC of heat source temperature. So, an experimental data collection has been provided in a field where there is a shortage of them.

Experimental results are compared against a theoretical model based on 1st and 2nd principles of thermodynamics. From this comparison, can be concluded that this kind of models are useful for thermodynamic cycle analysis but not for accurate energy analysis because heat transfer effects have important influence on them.

All the pairs have worked properly with the same facility (only the compressor has been changed to meet the proper displacement, and the electronic expansion valve controller has been programmed accordingly with the fluid used). No technical problems have arisen during the tests, that have been lasted for two months of continuously running for each pair of fluids.

Regarding to the R1270/R744 pair, the highest HTC compressor discharge temperatures are achieved in all the heat temperatures range tested, ranging from 7 to 12°C greater than those achieved with R134a, and very similar to those achieved in the LTC compressor. Also, the highest cooling capacity is achieved. However, slight COP decreases are measured respect to the R134a/R744 pair. So those results make R1270/R744 a good choice to upgrade the cooling capacity and recover energy from compressor discharge.

In respect to R290/R744 pair, it achieves better cooling capacity and energy efficiency results than R134a/R744 pair at low heat sink temperatures (20°C and 30°C), but it suffers a degradation on those parameters as sink temperature rises. So, at 40°C it worsens the energy efficiency and the cooling capacity values respect to R134a/R744. Considering the whole range tested, its energy behavior improves R134a/R744 at low and mid environmental temperatures and is neutral at warm ones.

As per the R600a/R744 pair, reductions between 1.6% and 6% in cooling capacity are obtained in comparison to R134a/R744 pair, as well as reductions from 4.4% to 7.7% in overall energy efficiency.

About the R1234ze(E) pair, the energy results are like those of R600a/R744, being reductions measured in overall energy efficiency around 8% in respect to R134a/R744, at the three heat sink temperatures tested, and neglecting variations in cooling capacity.

Regardless the energy behavior, the TEWI calculation demonstrates that all the refrigerants reduce the total CO2 equivalent emissions along the lifespan of the cascade refrigeration plant, what supposes an improve on the environmental performance.

To sum up, the four refrigerants tested against R134a paired with R744 in all cases, reduces the direct effect because of their low-GWP, but only R290 and R1270 do not increase the indirect effect respect to R134a. So, all of them, from an environmental point of view, could be considered for refrigeration plants, like the tested one. Due to the charge limits allowed by safety regulations, could be used in distributed refrigeration systems or in self-contained refrigeration freezing cabinets, either for industrial applications or commercial ones.

Declaration of Competing Interest

The authors declare no competing interests.

Acknowledgements

The authors gratefully acknowledge the Ministerio de Ciencia y Tecnología – Spain (project RTI2018-093501-B-C21) for financing this research work.

References

ASERCOM, "Refrigerant glide and effect on performances declaration," no. September, pp. 1–11, 2015, https://www.asercom.org/guides/#0a0edd2b641ef8307.

Catalán-Gil, J., Sánchez, D., Llopis, R., Nebot-Andrés, L., Cabello, R., 2018. Energy evaluation of multiple stage commercial refrigeration architectures adapted to F-gas regulation. Energies 11 (7) art, no, 1915. https://doi.org/10.3390/en11071915.

Coleman, H.W., Steele, W.G., 2018. Experimentation, Validation and Uncertainty Analysis For Engineers, 4th Edition. John Wiley & Sons, ISBN 978-1-119-41751-4.

DOE. U.S. Department of Energy, 2022, EnergyPlus version 22.1.0 https://energyplus.net/.

EPA. 2016. Transitioning to low-GWP alternatives (2016) https://www.epa.gov/sites/production/files/2016-12/documents/international_transitioning_to_low-gwp_alternatives_in_commercial_refrigeration.pdf.

European-Union, 2014, Regulation (EU) No 517/2014 of the European Parliament and of the Council of 16 April 2014 on fluorinated greenhouse gases and repealing Regulation (EC) No 842/2006, 2014.

Funder-Kristensen, T., Larsen, L.F.S., Thorsen, J.E., 2017. Integration of the hidden refrigeration capacity as heat pump in smart energy systems. In: Proceedings of the 12th IEA Heat pump conference. Rotterdam (Nederland).

IPCC/TEAP, 2015. Special report: safeguarding the ozono layer and the global climate system. Chapter 4 (2015). https://www.ipcc.ch/pdf/special-reports/sroc/sroc_full.pdf.

IPU. 2007. SecCool properties. https://www.ipu.dk/products/seccool/.

Iyer, S.R., Sankar, M., Ramakrishna, P.V., Sarangan, V., Vasan, A., Sivasubramaniam, A., 2015. Energy disaggregation analysis of a supermarket chain using a facility–model. Energy Build 97, 65–76.

JCGM, 2008. Joint Committee for Guides in Metrology, 2008 "JCGM 100 2008: evaluation of measurement data - guide to the expression of uncertainty in measurement.".

Kashra, M., Kody, M.P., 2021. Thermoeconomic evaluation and optimization of using different environmentally friendly refrigerant pairs for a dual-evaporator cascade refrigeration system. Processes **2021**, 9(10), 1855; https://doi.org/10.3390/pr9101855.

Lemmon E.W., Bell I.H., Huber M.L., McLinden M.O., 2018. NIST standard reference database 23: reference fluid thermodynamic and transport properties-REFPROP. Version 10.0. National Institute of Standards and Technology. Gaithersburg. Standard Reference Data Program.

Lund, Th, Skovrup, M.J., Holst, M., 2019. Comparing energy consumption and life cycle cost of industrial size refrigeration systems. In: Proceedings of the 25th IIR International Congress of Refrigeration: Montréal. Canada Manuscript ID: 947. https://doi.org/10.18462/iiricr.2019.0947.

Makhnatch, P., Mota-Babiloni, A., Khodabandeh, R., 2018. Energy evaluation of drop-in replacements for R134a in cascade CO2/R134a refrigeration units. Refrig. Sci. Technol. 1147–1153, 2018-June.

Moffat, R.J., 1985. Using uncertainty analysis in the planning of an experiment. J. Fluids Eng. Jun 1985, 107(2): 173-178. https://doi.org/10.1115/1.3242452.

Sanchez. D., Cabello. R., Llopis. R., Catalán-Gil. J., Nebot-Andrés L., 2019. Energy assessment and environmental impact analysis of an R134a/R744 cascade refrigeration plant upgraded with the low-GWP refrigerants R152a, R1234ze(E), propane (R290) and propylene (R1270), Int. J. Refrig., Volume 104, August 2019, Pages 321-334.

Morlet V. Coulomb D., Dupont J.L., 2017. The impact of the refrigeration sector on climate change. 35th Informatory Note on refrigeration technologies. IIF-IIR.https://iifiir.org/en/fridoc/the-impact-of-the-refrigeration-sector-on-climate-change-141135.

Tsamos, K.M., Amaris, C., Mylona, Z., Tassou, S., 2019. Analysis of typical booster configuration. Parallel-compressor booster configuration and R717/R744 cascade refrigeration system for food retail applications. Part 2: energy performance in various climate conditions. Energy Procedia 161, 268–274 March 2019. https://doi.org/10.1016/j.egypro.2019.02.091.

UNEP. 2016. 38th meeting of the open-ended working group (OEWG 38) of the parties to the Montreal Protocol on substances that deplete the ozone layer and 28th meeting of the parties to the Montreal protocol (MOP 28). Kigali 8. 10-14 October 2016.

Zhili, S., Qifan, W., Zhiyuan, X., Shengchun, L., Dandan, S., Qi, S., 2019. Energy and exergy analysis of low GWP refrigerants in cascade refrigeration system. Energy 170, 1170–1180.

Cabello R., Sánchez D., Llopis R., Catalán J., Nebot-Andrés L., Torrella E., 2017. Energy evaluation of R152a as drop in replacement for R134a in cascade refrigeration plants. Applied Thermal Engineering. Volume 110, 5 January 2017, Pages 972-984.